JOURNAL OF COMPUTATIONAL PHYSICS 25, 94–103 (1977)

Numerical Solution of a Two-Dimensional Vlasov Equation

MAGDI M. SHOUCRI AND RÉAL R. J. GAGNÉ

Department of Electrical Engineering, Laval University, Quebec, Canada

Received June 3, 1976; revised January 13, 1977

By means of a Hermite polynomials expansion in velocity space of the distribution function, the two-dimensional Vlasov equation is solved numerically by applying a multistep technique. We first study the case of a two-dimensional strongly nonlinear Landau damping, where a large amplitude oscillation is initially applied to the system. A second case is considered where an initially stable oscillation is applied to two-dimensional counter-streaming plasmas. The time evolution of these systems is studied and the performance of the numerical code is analyzed.

1. INTRODUCTION

A multistep technique for the numerical solution of a two-dimensional unmagnetized Vlasov equation has been recently presented [1], where preliminary results obtained by studying the two-dimensional free streaming case and the linearized Vlasov equation have been reported. It is the purpose of the present work to analyze the performance of the numerical code developed when it is applied for the solution of the nonlinear two-dimensional Vlasov equation. Two cases will be considered because of their physical relevance as well as to test the numerical code. We first study the time evolution of a two-dimensional strongly nonlinear Landau damping, when a large amplitude oscillation is initially applied to the system. The second case studied involves nonlinear plasma oscillations in two-dimensional counter-streaming plasmas when an initially decaying two-dimensional large amplitude oscillation is applied to the system. Linear theories predict the initial decay of a wave whose phase velocity lies on the negative slope of the distribution function. The additional effect of nonlinearly grown waves, especially when a large initial perturbation is applied, is a problem which is difficult to tackle theoretically. This effect is studied here by numerical methods and in our present case it is found that nonlinearly excited one-dimensional modes dominate the final state of the system.

Details on the numerical code developed have been given in [1]. In Section 2 we briefly indicate the main steps of the technique used in order to introduce the notation, and we also test the effect of the pseudocollision operator formally added to the Vlasov equation to eliminate the recurrence effect [1]. In Sections 3 and 4 we present the results obtained from the study of the strongly nonlinear Landau damping case and the streaming plasmas case. Section 5 will present our conclusion.

ISSN 0021-9991

2. The Pseudocollision Operator

We are solving the dimensionless equation

$$\frac{\partial f}{\partial t} + v_x \frac{\partial f}{\partial x} + v_y \frac{\partial f}{\partial y} + E_x(x, y, t) \frac{\partial f}{\partial v_x} + E_y(x, y, t) \frac{\partial f}{\partial v_y} = 0 \tag{1}$$

supplemented with Poisson's equation

$$\frac{\partial E_x}{\partial x} + \frac{\partial E_y}{\partial y} = \iint_{-\infty}^{\infty} f \, dv_x \, dv_y - 1. \tag{2}$$

The distribution function is expanded in velocity space using the expansion with the Hermite polynomials $H_{ev}(v_x)$ and $H_{e\mu}(v_y)$

$$f(x, y, v_x, v_y, t) = \frac{1}{2\pi} \sum_{\nu=0}^{\infty} \sum_{\mu=0}^{\infty} h_\nu h_\mu b_{\nu,\mu}(x, y, t) \, H_{ev}(v_x) \, H_{e\mu}(v_y) e^{-(1/2)(v_x^2+v_y^2)}. \tag{3}$$

When the series in Eq. (3) is inserted in Eqs. (1), (2), and the coefficients for the Hermite polynomials are collected, one obtains the infinite system of differential equations

$$\frac{\partial b_{\nu,\mu}}{\partial t} + \rho_\nu \left[\frac{\partial}{\partial x}(b_{\nu-1,\mu} + b_{\nu+1,\mu}) - E_x(x, y, t) b_{\nu-1,\mu}\right] + \rho_\mu \left[\frac{\partial}{\partial y}(b_{\nu,\mu-1} + b_{\nu,\mu+1}) - E_y(x, y, t) b_{\nu,\mu-1}\right] = 0, \tag{4}$$

$$\nabla^2 \phi = 1 - b_{0,0}(x, y, t), \tag{5}$$

where the potential ϕ is such that the electric field $\mathbf{E} = -\nabla\phi$. In Eq. (4) we have set $\rho_\nu = h_{\nu-1}/h_\nu$ and the ρ_ν are defined by the recursion relation

$$\rho_\nu \rho_{\nu+1} = \nu + 1. \tag{6}$$

Similar relations also apply to the coefficients ρ_μ.

Equation (4) is integrated numerically by splitting the equation into two parts and integrating it alternatively in the x and the y directions using a leapfrog scheme previously developed for the one-dimensional case [2–4]. To achieve the numerical solution, the infinite system in Eq. (4) is truncated at, say, $\nu = N_x$ and $\mu = N_y$ by arbitrarily setting

$$b_{N_x,N_y}(x, y, t) = 0. \tag{7}$$

This truncation results in a recurrence effect, which can be eliminated by formally adding a pseudocollision operator to the right-hand side of Eq. (1). We use an operator of the form [1]

$$\lambda C(v)^{2r+1} f + \eta \nabla^2 C(v)^{2r+1} f \tag{8}$$

where λ and η are constants, r is an integer, $C(v)$ is the two-dimensional Fokker–Planck operator

$$C(v) = \frac{\partial}{\partial v_x}\left(v_x + \frac{\partial}{\partial v_x}\right) + \frac{\partial}{\partial v_y}\left(v_y + \frac{\partial}{\partial v_y}\right) \tag{9}$$

and

$$\nabla^2 = \frac{\partial^2}{\partial x^2} + \frac{\partial^2}{\partial y^2}. \tag{10}$$

It is essential to test the effect of the operator in (8) on the solution, and at the same time one effects a further check to our numerical code. For this purpose Eqs. (1), (2) were solved with the initial condition

$$f(x, y, v_x, v_y, 0) = f_0(v_x, v_y)\, g(x, y) \tag{11}$$

where

$$f_0 = \frac{1}{2\pi} \exp\left(-\frac{v_x^2}{2} - \frac{v_y^2}{2}\right) \tag{12}$$

and

$$g(x, y) = 1 + A \cos k_x x \cos k_y y. \tag{13}$$

We choose $k_x = k_y = 0.25$ and $A = 0.05$. These conditions correspond to the presence of the two Fourier modes E_{xk} (0.25, 0.25) and E_{yk} (0.25, 0.25) at time $t = 0$.

The calculations were carried up to $t = 14.5$, using a time step $\Delta t = 0.05$, a mesh of 16×16 points (in order to provide an adequate representation of the higher modes) and 30×30 polynomials. We also used $\lambda = 18(2 \times 28)^{-3}$, $\eta = 5.5(2 \times 28)^{-3}$, and $r = 1$. The result for E_{xk} is shown in Fig. 1. The two modes E_{xk}(0.25, 0.25) and E_{yk}(0.25, 0.25) remained exactly equal in magnitude while the excited higher modes remained smaller than the fundamental modes by at least one order of magnitude.

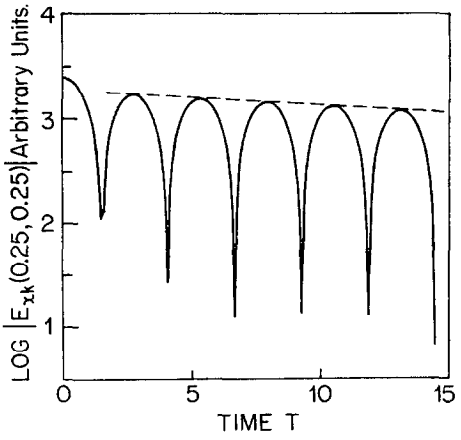

FIG. 1. Plot of the logarithmic value of E_{xk} against time, for the initial condition given in Eq. (11). The calculated values of ω/ω_p and γ/ω_p are, respectively, 1.208 and 0.0338.

The relative error in energy conservation was slightly less than 3×10^{-4}, and it took about 400 minutes of execution time (CPU time) for the calculations, using an IBM 370/168. The calculated real value of the frequency is $\omega/\omega_p = 1.208$ and the imaginary value (averaged over several peaks) is $\gamma/\omega_p = 0.0338$, while the corresponding theoretical values are $\omega/\omega_p = 1.220$ and $\gamma/\omega_p = 0.0343$, for $k = (k_x^2 + k_y^2)^{1/2} = 0.3535$. Hence, the agreement is very good and indicates that the damping constants λ and η are affecting the solution only slightly. The present values of λ and η are used for the calculations presented in Sections 3 and 4.

3. Strongly Nonlinear Landau Damping

Having tested the correctness of our scheme and the effect of the damping constants on the solution, attention is now directed to the case of a strongly nonlinear Landau damping. We take the same values of f_0 and $g(x, y)$ as are given in Eqs. (12) and (13), but with $A = 0.5$. The results are presented in Figs. 2–5. The two modes E_{xk} (0.25, 0.25) and E_{yk} (0.25, 0.25) remained exactly equal (up to the eighth decimal) for all values of t up to $t = 40.0$; this was also the case for the higher diagonal modes E_{xk} (0.5, 0.5) and E_{yk} (0.5, 0.5), and for the modes E_{xk} (0.75, 0.75) and E_{yk} (0.75, 0.75). There was a very slight difference occurring at fourth decimal (representing about 0.05%) between the nondiagonal modes E_{xk} (0.5, 0) and E_{yk} (0, 0.5), and the modes E_{xk} (0.75, 0.5) and E_{yk} (0.5, 0.75) (these four latter modes remained smaller in magnitude than the other modes by at least one order of magnitude or more). Figure 2 gives the plot, on a logarithmic scale of E_{xk} (0.25, 0.25) against time. A damping, which is stronger than the linear damping obtained in Fig. 1, is obserbed at the early evolution of the system; then a subsequent growth is observed up to $t = 30$. This behavior is similar to what one gets for the one-dimensional strongly nonlinear Landau damping

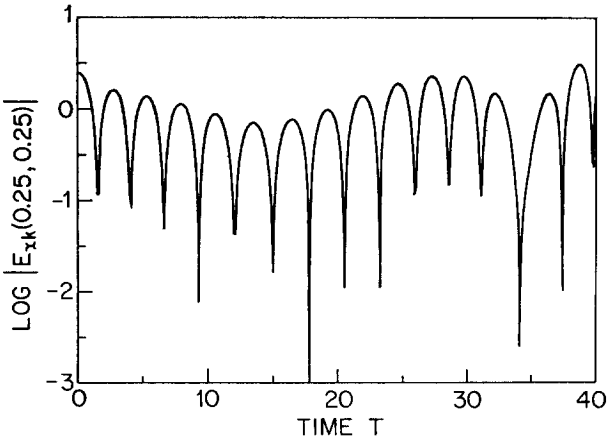

Fig. 2. Plot of the logarithmic value of E_{xk} (0.25, 0.25) against time, with the initial condition given in Eq. (11), with $A = 0.5$.

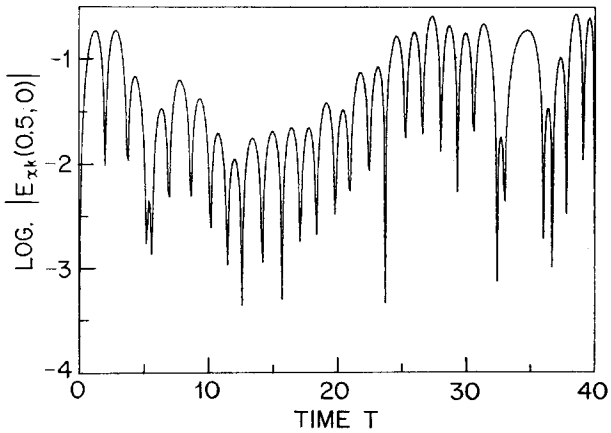

FIG. 3. Plot of the logarithmic value of E_{xk} (0.5, 0) against time. Same initial condition as in Fig. 2.

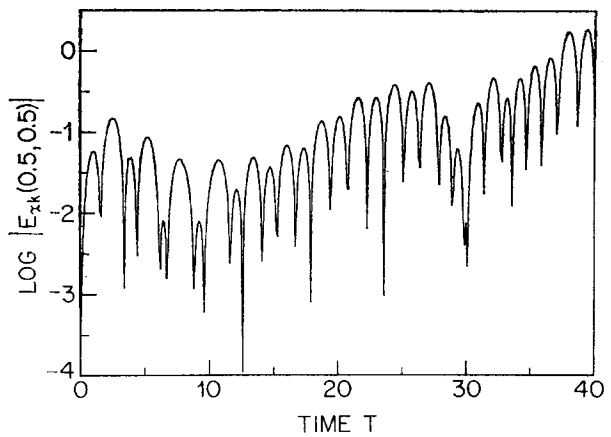

FIG. 4. Plot of the logarithmic value of E_{xk} (0.5, 0.5) against time. Same initial condition as in Fig. 2.

[2, 3]. The mode, however, does not seem to saturate and shows, rather, an oscillation from $t = 30$ to 40. The slight irregularity in the oscillation pattern which appears about $t = 34$ (and which is also apparent for the mode E_{xk} (0.5, 0) in Fig. 3) is probably due to small recurrence effects which have not been completely controlled by the pseudocollision operator. Neither for the fundamental mode, nor for the higher modes, in Figs. 3–5, does a steady state appear to have been reached, at $t = 40$. With the exception of the mode E_{xk} (0.5, 0.5) in Fig. 4 (which seems to reach together with E_{yk} (0.5, 0.5) at $t = 40$, a level close to the fundamental level for E_{xk} (0.25, 0.25) in Fig. 2) all the higher modes remained smaller than the fundamental modes by at least one order of magnitude. The two diagonal modes E_{xk} (0.5, 0.5) and E_{xk}

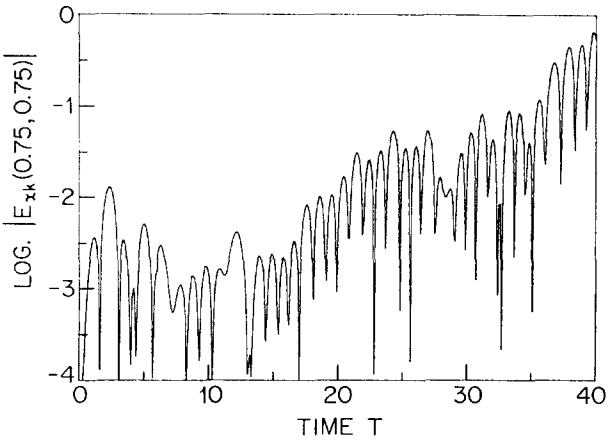

FIG. 5. Plot of the logarithmic value of E_{xk} (0.75, 0.75) against time. Same initial condition as in Fig. 2.

(0.75, 0.75) (in Figs. 4 and 5, respectively) show a similar evolution pattern in time, with local minima near $t = 9$ and $t = 30$, and a local maximum around $t = 25$.

The relative error in total energy conservation was about 10^{-2} at $t = 30$ (just before the slight distorsion due to recurrence appears). These results have been obtained using a mesh of 16×16 points and 30×30 polynomials, i.e., the equivalent of $(480)^2$ particles. The total time of execution (CPU time) was close to 18 hours and 48 minutes, using an IBM 370/168. This is equivalent to a computational effort of about 0.4 msec per "particle" per time step ($\Delta t = 0.05$).

4. COUNTER-STREAMING PLASMAS

In this case we study the time evolution of an initially decaying large amplitude oscillation in counter-streaming plasmas. The initial distribution function is taken as in Eq. (11), where f_0 is the double peaked Maxwellian

$$f_0(v_x, v_y) = \frac{v_x^2}{2\pi} \exp\left(-\frac{v_x^2}{2} - \frac{v_y^2}{2}\right) \tag{14}$$

and $g(x, y)$ is the same as in Eq. (13). We have used in this case $A = 0.25$. The electric field components E_x and E_y have, at $t = 0$, the Fourier components E_{xk} (0.25, 0.25) and E_{yk} (0.25, 0.25), respectively. These components are equal at $t = 0$ and remained equal for all time t (together with their complex conjugates).

Figure 6 shows the plot of the logarithm of the absolute value of the mode E_{xk} (0.25, 0.25), excited at $t = 0$. It indicates at the beginning that the system is oscillating at two linearly independent frequencies having a relative phase of 180° and decaying exponentially. At this early evolution of the system most of the energy is

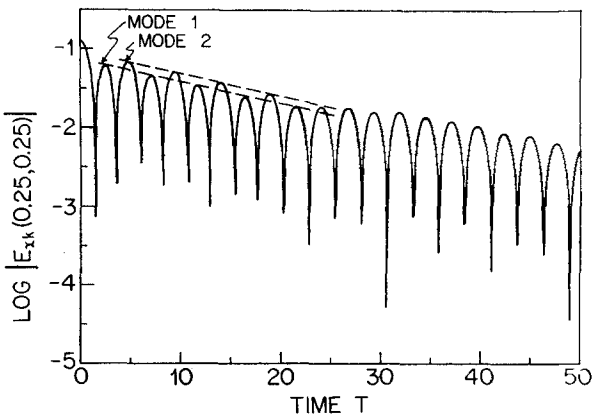

FIG. 6. Plot of the logarithmic value of E_{xk} (0.25, 0.25) against time, with the initial condition in Eq. (14) with $A = 0.25$.

concentrated in the fundamental modes E_{xk} (0.25, 0.25) and E_{yk} (0.25, 0.25), so that the total electric energy in Fig. 8 shows clearly on a linear scale the exponential decay in time accompanied by oscillations at the two frequencies (called mode 1 and mode 2 on Fig. 8). The period of oscillation of these two modes was exactly equal to 9.2 ω_p^{-1}. For a perturbation with a wavenumber $k = 0.25 \times 2^{1/2}$, this leads to a phase velocity well on the negative slope of the distribution function as given by Eq. (14) and, hence, implies damping. The damping rates, averaged over the first peaks, were respectively, 0.0626 and 0.0655 (the results are not accurate enough to determine whether the damping rates are exactly equal). As was previously mentioned the mode E_{yk} (0.25, 0.25) remained exactly equal to E_{xk} (0.25, 0.25) for all time t (this equality was verified up to the eighth decimal). The diagonal modes E_{xk} (0.5, 0.5), E_{xk} (0.75, 0.75) were also excited and remained, respectively, equal to the diagonal modes

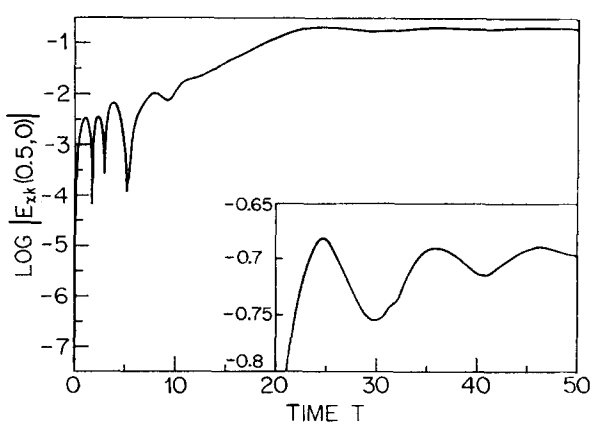

FIG. 7. Plot of the logarithmic value of E_{xk} (0.5, 0) against time. Same initial condition as in Fig. 6.

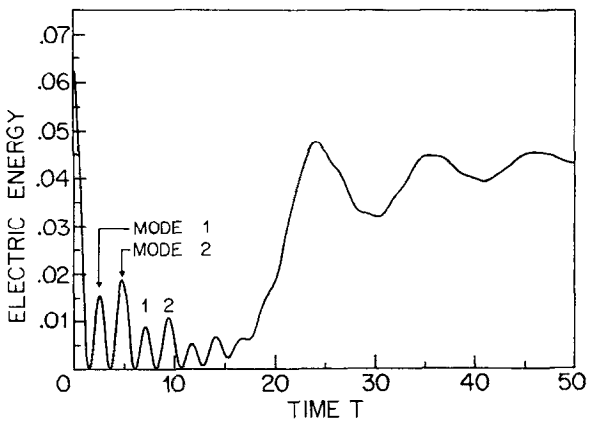

FIG. 8. Plot of the electric energy against time. Same initial condition as in Fig. 6.

E_{yk} (0.5, 0.5), E_{yk} (0.75, 0.75) for all time t (they were however, at least two order of magnitudes smaller than the fundamental mode E_{xk}). The history of the nondiagonal modes is different. Figure 7 shows the evolution of the one-dimensional mode E_{xk} (0.5, 0). This nonlinearly excited mode shows a one-dimensional instability which, for counter-streaming plasmas, is characteristic of a perturbation whose phase velocity falls on the positive slope of the distribution function. This perturbation drives the electric energy wave in Fig. 3 to a typical two-stream instability behavior characterized by an exponential growth for $t > 15$ followed by saturation, and, then, trapped particles oscillations. That these trapped particle oscillations are due to the one-dimensional mode E_{xk} (0.5, 0) can be easily verified by considering the peaks and valleys of the electric field energy curve in Fig. 8 which, for $t > 20$, closely follow those of the curve of the mode E_{xk} (0.5, 0) (which has been plotted with a magnified scale in the lower box of Fig. 7). Figure 9 shows another one-dimensional

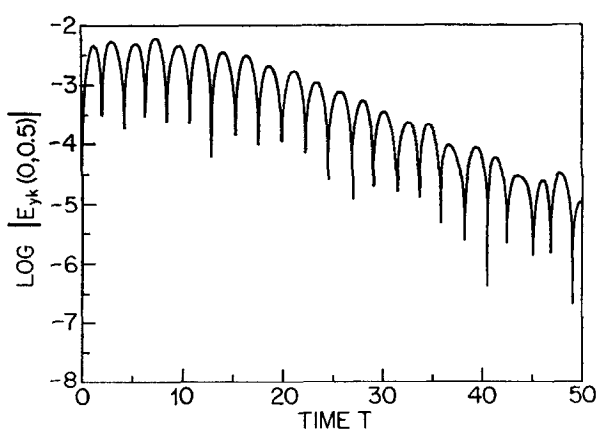

FIG. 9. Plot of the logarithmic value of E_{yk} (0, 0.5) against time. Same initial condition as in Fig. 6.

mode, the mode E_{yk} (0, 0.5). This mode has a very small initial growth followed by a continuous decay; as can be easily verified, the evolution of the two nondiagonal modes E_{xk} (0.5, 0) and E_{yk} (0, 0.5) is totally different. Finally, Fig. 10 shows a one-dimensional mode excited in the x direction, the mode E_{xk} (0.25, 0). It shows a continuous growth from a very low initial level; this mode, however, and all the other modes, remain at $t = 50$ at least two order of magnitudes lower than the mode E_{xk} (0.5, 0).

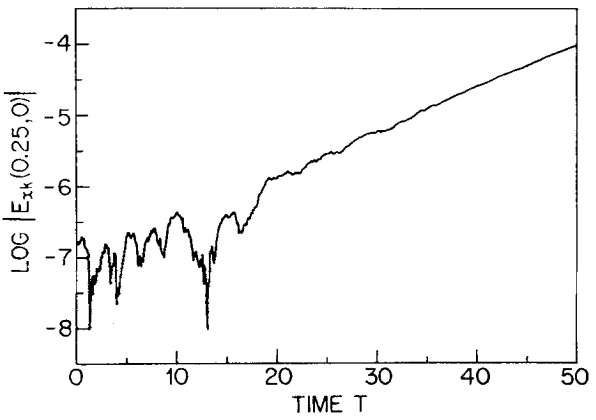

FIG. 10. Plot of the logarithmic value of E_{xk} (0.25, 0) against time. Same initial condition as in Fig. 6.

At $t = 50$, after 800 time- steps, the relative error in energy conservation was 1.5×10^{-3}. The execution time (CPU time) was about 23 hours, using an IBM 370/168. These calculations were done with 30×30 polynomials and a mesh of 16×16 points, i.e., the equivalent of $(480)^2$ "particles." This corresponds to a computational effort of about 0.4 msec per particle per time-step ($\Delta t = 0.05$).

5. CONCLUSION

In the present work, we have tested a numerical code for the solution of a two-dimensional Vlasov equation, using a multistep technique [1]. The results indicate that the code in its present form is accurate. A typical figure for the relative error in energy conservation for the solution of nonlinear problems is 10^{-2} to 10^{-3}. Comparison with available theoretical results from the linear theory gives very good agreement (the error is about 1 % for the result in Fig. 1). Nonlinear effects have been studied with a matrix of 30×30 polynomials and a mesh of 16×16 points, i.e., the equivalent of $(480)^2$ particles. This is equivalent to the simulation of one-dimensional nonlinear effects with 480 particles, which is the optimized result reported for the one-dimensional case in [2–4]. The typical computational effort is about 0.4 msec per particle per time step (using a time-step $\Delta t = 0.05$, and an IBM 370/168).

The code has been applied to study the time evolution of a two-dimensional strongly nonlinear Landau damping, and the time evolution of a decaying oscillation in counter-streaming plasmas. The physical results are interesting and new. In both cases, the corresponding diagonal modes in the x and y directions remained exactly equal for all time. The case of a strongly nonlinear Landau damping, when a large amplitude oscillation is initially applied to the system, shows the fundamental mode growing again after the initial decay (see Fig. 2), a behavior indicating the formation of a positive slope in the distribution function. The case of an initially decaying two-dimensional oscillation in counter-streaming plasmas shows a single one-dimensional mode, excited nonlinearly, driving a two-stream instability and giving, as a final state, a behavior typical of one-dimensional trapped particle oscillations; this asymptotic behavior differs from the results obtained in earlier particle simulations [5], where several initially unstable two-dimensional modes lead to an asymptotic solution of the electric field energy showing a smooth decay in time after saturation, without trapped particle oscillations. This difference is due to the fact that in the present case, we have a single one-dimensional mode dominating the asymptotic state of the system.

In addition to the results discussed in Fig. 1, testing the code for different mesh sizes has been reported in [1] for the linear case. This has not been effected for the nonlinear problem, but recent results obtained with a new code [6] using splitting schemes, do show very good agreement with the present code for the nonlinearly grown waves.

Acknowledgments

The authors are grateful to the "Direction de l'Enseignement Supérieur" for special permission to use the IBM 370/168 of the Ministry of Education of the Provincial Government of Quebec (SIMEQ) as well as to the SIMEQ authorities, who made it possible to perform the present calculations. M. Shoucri is grateful to Professor G. Knorr for many fruitful discussions.

References

1. M. Shoucri and R. R. J. Gagné, *J. Computational Phys.* **23** (1977), 242.
2. M. Shoucri and R. R. J. Gagné, *J. Computational Phys.* **21** (1976), 238.
3. G. Knorr, *J. Computational Phys.* **13** (1973), 165.
4. M. Shoucri and G. Knorr, *J. Computational Phys.* **14** (1974), 84.
5. R. L. Morse and C. W. Nielson, *Phys. Rev. Lett.* **23** (1969), 1087.
6. M. Shoucri and R. R. J. Gagné, Splitting schemes for the numerical solution of a two-dimensional Vlasov equation, *J. Computational Phys.*, in press.